We P1 13

Viscoelastic Full Waveform Inversion of Sea Bottom Long Offset Seismic Data in Presence of Attenuation

T. Belahi* (Institut de Physique du Globe de Paris (IPGP)), S.C. Singh (Institut de Physique du Globe de Paris (IPGP)) & N. Fuji (Institut de Physique du Globe de Paris (IPGP))

SUMMARY

Seismic data acquired at the sea bottom are more and more available. It is now possible to record shear and converted waves thanks to this type of data. It opens up the possibility to constrain bot h P- and S-wave velocities with tools such as full waveform inversion (FWI). The data recorded at the sea bottom can be particularly sensitive to attenuation, especially at long-offset, thus often viscoelastic FWI is required. In this study we use a 2D viscoelastic FWI scheme on synthetic data to assess possibility to treat the attenuation parameters as passive parameters of the inversion and still recover acceptable models for P- and S-wave velocities. Alternatively, we assess the inversion of the seismic velocities as well as the parameters controlling attenuation altogether. We find that inverting for all parameters together is necessary to get access to the short wavelength features of the subsurface model because the short-wavelength attenuation model is required to properly treat reflections and converted waves close to the critical angle. Inverting long-offset data in conjugation with a smooth attenuation model is sufficient to yield the long wavelength features of the velocity models.

Introduction

Full waveform inversion (FWI) of seismic data became a standard tool in applied geophysics for estimating the parameters of the subsurface. The acoustic and elastic formulations of FWI have been proved successful in various geological settings. However, in presence of seismically attenuating geological features such as gas clouds, hydrate bearing sediments or unconsolidated sediments, acoustic or elastic FWI fail to yield meaningful results. This issue can be addressed by using viscoelastic FWI, implemented either in time-domain or in frequency domain. Although the frequency-domain approach is much easier to implement, the time-domain approach is interesting as is probes the full frequency band of the data and not only a selected number of frequencies. Furthermore, we prefer the time-domain approach under the existence of squirt-flow, for example, where the attenuation mechanism at stake is frequency dependent (Quintal et al., 2012).

Inverting for seismic velocities in presence of attenuation is challenging, since it is difficult to distinguish, especially from long-offset data, the attenuation and elastic parameter effects on waveform data (Belahi et al., 2015). However, relying on a passive implementation of attenuation, i.e. an inversion scheme, where one does not update the information on the parameters controlling the intrinsic attenuation, proved to be relatively robust for viscoacoustic FWI (Kurzman et al., 2013). More and more ocean bottom cable data are available, which enable to invert for both P- an S-wave velocities. It can greatly improve subsurface characterization. In this paper, we assess if the passive inversion of both P- and S-wave velocities, within a viscoelastic time-domain FWI scheme, is also robust, or if inverting for both velocities and the quality factors controlling attenuation yield better results. We compare both approaches on a modified version of the Marmousi-2 model (Martin et al., 2002).

Method

Full waveform inversion is local optimization method based on minimizing the least-squares difference between observed and synthetic data by iteratively computing a gradient direction that optimize the model (Lailly, 1983). In order to properly account for attenuation, one needs to model the effects of attenuation in the forward modeling. We use linear viscoelasticity to model attenuation, based on a general formulation of Hooke's law, which introduces a time-dependence between strain and stress:

$$\sigma^{ij}(\mathbf{x},t) = \int_{-\infty}^{\infty} \Psi^{ijkl}(\mathbf{x},t-\tau)\epsilon^{kl}(\mathbf{x},t)d\tau\,, \tag{1}$$

where σ^{ij} is stress, ϵ^{kl} is strain and Ψ^{ijkl} is the time-dependent stiffness tensor. We use Standard Linear Solids (SLS) to parameterize the stiffness tensor (Robertsson et al., 1994). This allows us to replace the convolution equations by a set of ordinary partial differential equations, introducing memory variables that account for the dissipation of energy over the propagation of the viscoelastic wavefield. In this study, each cell of the model is parameterized by a single SLS. It directly maps the seismic velocities (Vp, Vs) and the quality factors (Qp, Qs) to the Lamé parameters required for the modeling.

At each iteration of the inverse problem, the model is updated based on the gradient direction. We compute the gradient for four parameters: $\pi = \lambda + 2\mu$, μ at time 0^+ and $\Delta\pi$, which account for the variation of π and μ over the propagation time. The resulting gradient for π is:

$$\delta\pi(\mathbf{x},0^+) = -\int_{t_0}^{t_1} dt \overleftarrow{\epsilon^{ii}}\overrightarrow{\epsilon^{jj}}(\mathbf{x},t) \text{ and } \delta\Delta\pi(\mathbf{x}) = -\int_{t_0}^{t_1} dt \overleftarrow{\epsilon^{ii}}\overrightarrow{r^{jj}}(\mathbf{x},t)\,, \tag{2}$$

where r^{kl} corresponds to the memory variables governed by first order partial differential equations (Tarantola, 1988). The gradients on the Lamé parameters can then be mapped to set of parameters Vp, Vs, Qp and Qs, such that:

$$\begin{pmatrix} \delta Vp \\ \delta Vs \\ \delta Qp \\ \delta Qs \end{pmatrix} = \begin{pmatrix} 2\rho Vp & 0 & \frac{2d\rho Vp}{Qp-c} & 0 \\ 0 & 2\rho Vs & 0 & \frac{2d\rho Vs}{Qs-c} \\ 0 & 0 & -\frac{dVp^2\rho}{(Qp-c)^2} & 0 \\ 0 & 0 & 0 & -\frac{dVs^2\rho}{(Qs-c)^2} \end{pmatrix} \begin{pmatrix} \delta\pi \\ \delta\mu \\ \delta\Delta\pi \\ \delta\Delta\mu \end{pmatrix}, \quad (3)$$

where c and d can be expressed in terms of the characteristic relaxation times of the SLS for each cell of the model.

Experimental setting

In order to assess the need for inverting for the attenuation parameters or not, we used a modified version of the Marmousi-2 model where Qp and Qs are correlated to Vp over Vs ratio and range, respectively, from 20 to 150 and 10 to 120. Here in this study, we run two synthetic inversions: one with attenuation considered as passive parameters ("passive inversion") and another inverted for all the four parameters, Vp, Vs, Qp, Qs ("active inversion"). In the first experiment, we invert only for P- and S-waves velocities and do not update the model for Qp and Qs. At each iteration we use L-BFGS to determine a model perturbation based on the gradients of Vp and Vs, this perturbation is then used in a line-search algorithm to determine the step length for the model update (Brossier et al., 2009). In the second experiment, the four parameters Vp, Vs, Qp and Qs are updated at each iteration. We provide the perturbation for the line-search algorithm in order to cope with the different sensitivities between velocities and quality factors. For both experiments, we first invert in the frequency band of 0-3.5 Hz and then in the higher frequency band of 0-5.5 Hz. The inversions use 62 shots spaced by 250 m each, 351 receivers spaced by 25 m each and lying on the sea bottom spanning 8.75 km. We inverted for the pressure component and data window is set to be 5 s. The modeling grid used for these experiments is discretized on 6.25 m by 6.25 m grid and the time-step increment is 0.5 ms. Figure 1 shows the true model and starting Vp models used for both experiments. The observed data are generated with a 7.5 Hz Ricker wavelet, which is also the resonant frequency for the SLSs parameterizing Qp and Qs.

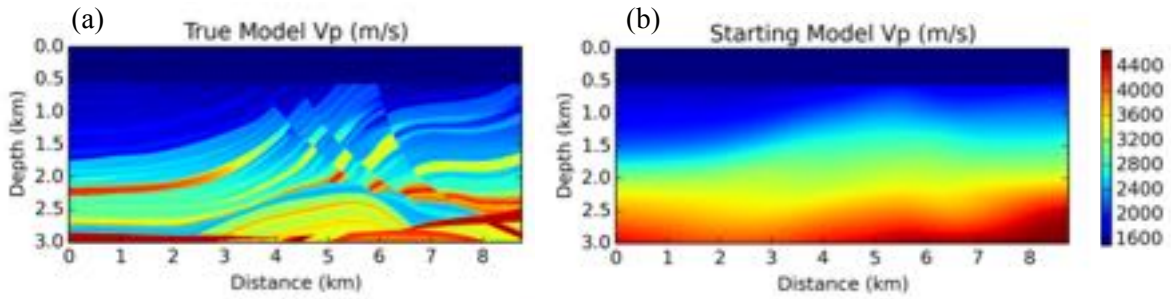

Figure 1 *True (left) and starting (right) models for P-wave velocity (Vp).*

Results

Figure 2a shows the final P-wave velocity model obtained in the first experiment, inverting only for P- and S-wave velocities, in the frequency band of 0 to 3.5 Hz. The results are close to the velocity model we obtain by inverting for the four parameters Vp, Vs, Qp and Qs shown, for P-waves velocities, in the Figure 2b. Both experiments share the same starting model, shown in Figure 1b, and yield a similar reduction of the initial misfit. These two models are then used as the starting models to invert for the data in the frequency band of 0 to 5.5 Hz. Figures 2c and 2d show the final results for

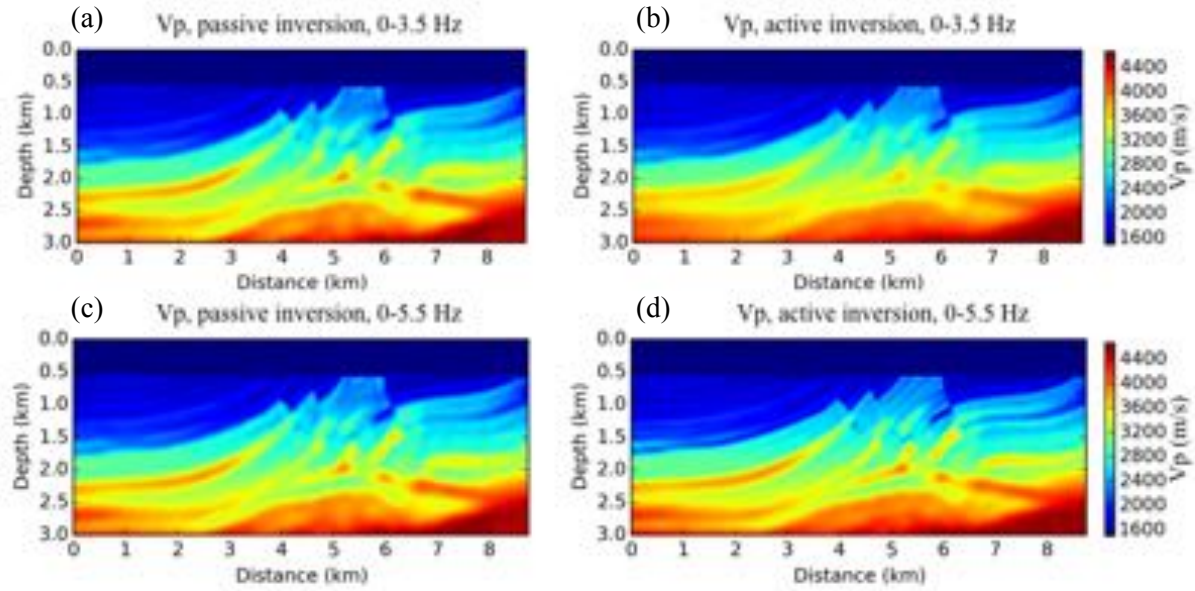

Figure 2 *(a) P-wave velocity models obtained by inverting only for P- and S-wave velocities in the 0 - 3.5 Hz band. (b) P-wave velocity model obtained by inverting both for velocities and quality factors in the 0 - 3.5 Hz band. (c) P-wave velocity models obtained by inverting only for P- and S-wave velocities in the 0 - 5.5 Hz band with (a) as a starting model. (d) P-wave velocity model obtained by inverting both for velocities and quality factors in the 0 - 5.5 Hz band with (b) as a starting model.*

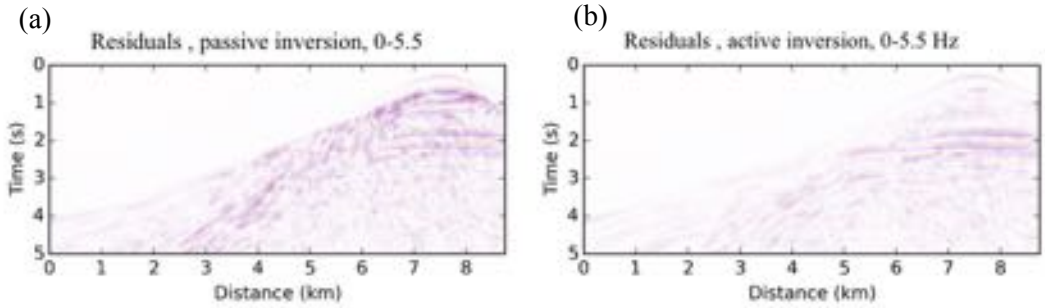

Figure 3 *Final residuals when inverting only for P- and S-wave velocities with a smooth attenuation background (a) and when inverting for both seismic velocities and the quality factors (b).*

the P-wave velocities for the inversion of velocities only and the inversion of the four parameters respectively. We cannot observe a significant improvement by increasing the frequency band, while inverting only for P- and S-waves velocities and the inversion converged to a local minimum. This can be seen by comparing Figure 2c with Figure 2a. The increase of the frequency band, while inverting for the four parameters, does yield improvement on the resolution of the different layers. This is especially true in the upper part of the model. For instance, the low velocity anomaly located at the point (x,z) = (6 km, 1.2 km) is much better resolved in Figure 2d than in Figure 2b or Figure 2c.

Figure 3 compares the final residuals obtained after the inversions performed in the frequency band of 0 to 5.5 Hz. The degree of residuals on the first arrival at long offset is equivalent in both Figure 3a and Figure 3b. The main differences are observed on the reflection arrivals both at short offset and close to the critical angle. This is true for the PP arrivals and the PSP arrivals. This means that a smooth attenuation model is sufficient to represent the impact of attenuation on the refracted waves, especially at low frequencies. At higher frequencies, when attenuation play a greater role, a smooth model for attenuation cannot represent the attenuation effects on reflected and converted waves. Inverting for attenuation allows us to properly treat the PSP arrivals, which yield an improved S-wave velocity model as shown in Figure 4b compared to one we get without inverting for attenuation in Figure 4a. The models recovered for Qp and Qs are respectively shown in Figure 5a and Figure 5b.

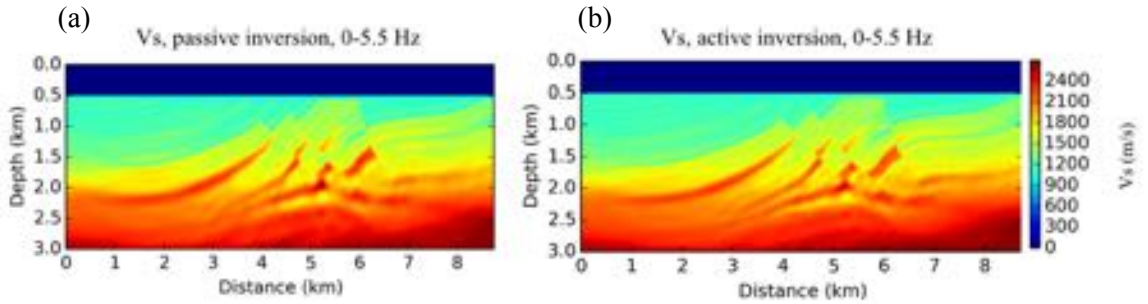

Figure 4 *Final Vs models for passive inversion (a) and active inversion (b)*

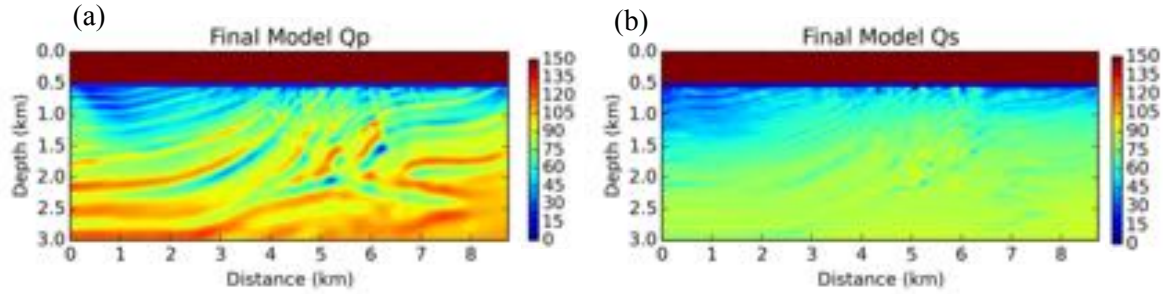

Figure 5 *Final Qp model (a) and Qs model (b) for the active inversion.*

Conclusion

We conducted a study based on viscoelastic FWI implemented in 2D in order to assess the need for inverting for attenuation and deriving a model that accounts for contrast in attenuation when inverting data that are acquired in an area of strong attenuation and when information on S-wave velocities is contained in the data. It appears that a smooth attenuation background is only sufficient for inverting long offset refracted waves and extract the long wavelengths information from the data. The data at mid-offset, close to the critical angle, depends very much on the attenuation contrast in the models, thus it is necessary to invert for both velocities and quality factors to properly account for this part of the data which grant access to the shorter wavelengths of the model.

Acknowledgements

The research described in this abstract was carried out as a part of the Paris Exploration Geophysics group project (GPX) funded by the French National Research Agency (ANR), CGG, Schlumberger and Total. Numerical computation were performed on the S-CAPAD platform at IPGP.

References

Belahi, T., Fuji, N., & Singh, S. C. [2015] Elastic Versus Viscoelastic Full Waveform Inversion of Near-offset and Wide-angle Data in the Presence of Attenuation. *77th EAGE Conference and Exhibition 2015,* p. 1–4

Kurzmann, A., Przebindowska, A., Kohn, D., & Bohlen, T. [2013] Acoustic full waveform tomography in the presence of attenuation: a sensitivity analysis. *Geophysical Journal International*, **195**(2), p985–1000

Lailly, P. [1983] The seismic inverse problem as a sequence of before stack migration. *Conference on Inverse Scattering, Theory and Applications, SIAM, Expanded Abstracts*, 206-220

Martin, G. S., Marfurt, K. J., & Larsen, S. [2002] Marmousi-2: An updated model for the investigation of AVO in structurally complex areas. *SEG Technical Program Expanded Abstracts*, **21**(1), 1979–1982.

Quintal, B., Steeb, H., Frehner, M., Schmalholz, S. M., & Saenger, E. H. [2012] Pore fluid effects on S-wave attenuation caused by wave-induced fluid flow. *Geophysics*, **77**(3), L13–L23

Robertsson, J. O. a., Blanch, J. O. and Symes, W. W. [1994] Viscoelastic finite-difference modeling. Geophysics, **59**(9)

Tarantola, A. [1988] Theoretical Background for the Inversion of Seismic Waveforms, Including Elasticity and Attenuation. *Pure and Applied geophysics*, **128**, p365-399